Journal of Solid State Chemistry 184 (2011) 1355–1360

Contents lists available at ScienceDirect

Journal of Solid State Chemistry

journal homepage: www.elsevier.com/locate/jssc

Effect of ring coordination of pyridine-3,5-dicarboxylate and metatungstate to *Ln* ions on metatungstate structure: Synthesis, structure and optical property of four new compounds

Dan-Dan Liu, Ya-Guang Chen*, Chun-Jing Zhang, Hua-Xin Meng, Zhi-Chao Zhang, Chun-Xia Zhang

Key Laboratory of Polyoxometalates Science of Ministry of Education, College of Chemistry, Northeast Normal University, Changchun 130024, PR China

ARTICLE INFO

Article history:
Received 12 January 2011
Received in revised form
20 March 2011
Accepted 27 March 2011
Available online 8 April 2011

Keywords:
Lanthanide complexes
Organic–inorganic hybrid
Polyoxometalate
Luminescent property

ABSTRACT

Four novel compounds based on α-metatungstate $[H_2W_{12}O_{40}]^{6-}$ (W_{12}) and *Ln*–organic complexes, $(NH_4)_4[Ln_2(L)_2(H_2O)_9(H_2W_{12}O_{40})]\cdot nH_2O$ (Ln=Eu^{III} (**1**), Gd^{III} (**2**), Dy^{III} (**4**), $n=11$; Tb^{III} (**3**), $n=12$; L=pyridine-3,5-dicarboxylate dianion) have been synthesized in aqueous solution and characterized by element analysis, IR spectrometry and thermogravimetric analysis. Single-crystal X-ray diffraction analyses reveal these compounds are isostructural with a $P21/n$ space group. The W_{12} cluster acting as a tridentate ligand connects three Ln^{3+} ions, in turn, each *Ln*2 ion links two W_{12} clusters, as a result, a W_{12}–*Ln* polymeric chain is formed. Coordination of pyridine-3,5-dicarboxylate ligands to the Ln^{3+} ions leads to a *Ln*–L polymeric chain. The two chains, W_{12}–*Ln* and *Ln*–L, share *Ln*2 ions, resulting in a 2-D layer. Ring coordination of pyridine-3,5-dicarboxylate and W_{12} to the *Ln* ions changes some bond angles of W_{12} that leads to a slight distortion of W_{12} and splitting of vibration band of W–Oc–W. Solid-state photoluminescence properties of compounds **1**–**4** have been investigated.

1. Introduction

In recent years, increasing attention has been turned to the design and synthesis of lanthanide-based metal-organic frameworks (MOFs) due to their coordination characteristics and exceptional optical and magnetic properties [1–6]. Compared to transition metals, lanthanides have higher coordination numbers and more flexible coordination geometry, which make it difficult to control the preparation of lanthanide complexes but are useful in the formation of MOF architectures [7–9]. On the other hand, most of the lanthanide compounds exhibit characteristics of photophysical properties, which can contribute to *f*–*f* transitions with an extremely narrow bandwidth [10]. Integrating with the above two points, the MOFs based on lanthanides have great potential applications, such as catalysis, adsorption, magnetic materials, separation sensors, luminescent sensors, etc. [11–14].

It is well known that polyoxometalates (POMs), a unique class of metal-oxide clusters, can provide a large number of terminal and bridging oxygen atoms and be used as multi-dentate inorganic ligands [15]. In this field, a branch is to construct multi-dimensional organic–inorganic hybrid materials via combination of POMs with MOFs [16–18]. Among the various types of polyanions, the α-metatungstate polyanion $[H_2W_{12}O_{40}]^{6-}$ (W_{12}) possess higher charge density and some structural features, and can provide a variety of possibilities of intermolecular linkages [19–21]. Hence, the construction of high-dimensional hybrid materials based on the W_{12} clusters and *Ln* coordination complexes is a research topic. However, the judicious choice of the organic linker plays a key role in the synthesis of lanthanide-based POMs. Among those organic ligands, the pyridinecarboxylic acids, such as pyridine-2,6-dicarboxylic acid, pyridine-4-carboxylic acid, etc., have been investigated widely, but the multi-dimensional structure compound constructed by rare earth elements, POMs and pyridine-3,5-dicarboxylic acid (H_2L) has not been reported. Hence, we employ pyridine-3,5-dicarboxylic acid as organic ligand based on the following considerations: (i) the flexibility and multifunctional coordination sites of pyridine-3,5-dicarboxylic acid may generate multidimensional structures; (ii) it can be deprotonated to HL^- and L^{2-}, which provide more coordination modes and (iii) the different position of the carboxyl groups in pyridine-3,5-dicarboxylic acid may make the ligand have different coordination modes comparing with that of pyridine-2,6-dicarboxylic acid.

Based on the above mentioned points, we have chosen W_{12} clusters as building blocks and *Ln*–H_2L coordination complexes as linkers to construct the multidimensional POM-based hybrid materials with conventional solution method. Herein, we report the synthesis, structures and properties of four new compounds, $(NH_4)_4[Ln_2(L)_2(H_2O)_9(H_2W_{12}O_{40})]\cdot nH_2O$ (Ln=Eu^{III} (**1**), Gd^{III} (**2**), Dy^{III} (**4**), $n=11$; Tb^{III} (**3**), $n=12$; L^{2-}=pyridine-3,5-dicarboxylate dianion).

---

* Corresponding author.
E-mail address: chenyg146@nenu.edu.cn (Y.-G. Chen).

0022-4596/$ - see front matter © 2011 Elsevier Inc. All rights reserved.
doi:10.1016/j.jssc.2011.03.047

2. Experimental section

2.1. Materials and general methods

The lanthanide (III) nitrates were prepared by dissolving corresponding lanthanide oxides in nitric acid and followed by recrystallization and drying. $(NH_4)_6[H_2W_{12}O_{40}]\cdot 3H_2O$ was synthesized according to the literature and characterized by IR spectroscopy and TG analyses [22]. All other chemicals were obtained from commercial sources and used without further purification. W, Eu, Gd, Tb and Dy were determined by a Leaman inductively coupled plasma (ICP) spectrometer. IR spectra were recorded in the range 400–4000 cm^{-1} on a Magna-560 spectrophotometer using KBr pellets. The Ammonium–N was determined by ion chromatography (DIONEX 100 with DIONEX CDM-1). TG analyses were performed on a Pyris Diamond (Perkin-Elmer) instrument in N_2 atmosphere with a heating rate of 10 °C min^{-1}. The fluorescent spectra of **1** and **4** were measured on an F-7000 FL Spectrophotometer and compounds **2** and **3** were measured on a FLSP920 Edinburgh Fluorescence Spectrophotometer.

2.2. Syntheses of **1–4**

2.2.1. Synthesis of $(NH_4)_4[Eu_2(L)_2(H_2O)_9(H_2W_{12}O_{40})]\cdot 11H_2O$ (**1**)

H_2L (0.0340 g, 0.2 mmol) was dissolved in 10 cm^3 hot water. Then 10 cm^3 aqueous solution of $Eu(NO_3)_3\cdot 6H_2O$ (0.0342 g, 0.10 mmol) was added into the above solution. After the mixed solution was stirred for 50 min at about 70 °C, $(NH_4)_6[H_2W_{12}O_{40}]\cdot 3H_2O$ (0.3006 g, 0.1 mmol) was added into the solution. After stirred for one hour, the solution was filtered and the filtrate (pH=2.1) was allowed to evaporate in air at room temperature. After about 1 week, colorless block crystals of **1** suitable for X-ray diffraction were obtained. Anal. Found for **1**: C, 4.18; H, 1.71; N, 2.04; Eu, 7.68; W, 56.49 (%); $C_{14}H_{64}N_6O_{68}Eu_2W_{12}$ (Mr=3914.40, 43% based on Eu) requires C, 4.30; H, 1.63; N, 2.15; Eu, 7.77; W, 56.36 (%). ν_{max}(KBr pellet) cm^{-1}: 3424.27(s), 1641.41(m), 1575.19(m), 1439.09(m), 1397.32(m), 1286.31(w), 1108.84(w), 936.19(m), 877.16(m), 780.83 (m), 752.89(m), 421.79(m).

2.2.2. Synthesis of $(NH_4)_4[Gd_2(L)_2(H_2O)_9(H_2W_{12}O_{40})]\cdot 11H_2O$ (**2**)

An identical procedure with **1** was followed to prepare **2** except $Eu(NO_3)_3\cdot 6H_2O$ was replaced by $Gd(NO_3)_3\cdot 6H_2O$. After about one week, colorless block crystals of **2** suitable for X-ray diffraction were obtained. Anal. Found for **2**: C, 4.15; H, 1.54; N, 2.29; Gd, 8.19; W, 55.08 (%); $C_{14}H_{64}N_6O_{68}Gd_2W_{12}$ (Mr=3924.96, 45% based on Gd) requires C, 4.28; H, 1.63; N, 2.14; Gd, 8.01; W, 56.21 (%). ν_{max} (KBr pellet) cm^{-1}: 3432.44(s), 1642.81(s), 1579.18(s), 1442.39(m), 1397.91(s), 1286.43(w), 1107.90(w), 937.75(s), 877.48(s), 782.47(s), 753.71(s), 421.89(w).

2.2.3. Synthesis of $(NH_4)_4[Tb_2(L)_2(H_2O)_9(H_2W_{12}O_{40})]\cdot 12H_2O$ (**3**)

An identical procedure with **1** was followed to prepare **3** except $Eu(NO_3)_3\cdot 6H_2O$ was replaced by $Tb(NO_3)_3\cdot 6H_2O$ and the amount of $(NH_4)_6[H_2W_{12}O_{40}]\cdot 3H_2O$ (0.1506 g, 0.05 mmol). After about one week, colorless block crystals of **3** suitable for X-ray diffraction were obtained. Anal. Found for **3**: C, 4.12; H, 1.84; N, 2.28; Tb, 7.97; W, 56.02 (%); $C_{14}H_{66}N_6O_{69}Tb_2W_{12}$ (Mr=3946.32, 44.1% based on Tb) requires C, 4.26; H, 1.67; N, 2.13; Tb, 8.05; W, 55.90 (%). ν_{max}(KBr pellet) cm^{-1}: 3420.71(s), 1643.67(s), 1580.05(s), 1442.39(m), 1398.27 (s), 1286.39(w), 1108.90(w), 983.42(s), 877.13(s), 782.78(s), 753.66(s), 421.82(m).

2.2.4. Synthesis of $(NH_4)_4[Dy_2(L)_2(H_2O)_9(H_2W_{12}O_{40})]\cdot 11H_2O$ (**4**)

An identical procedure with **1** was followed to prepare **4** except $Eu(NO_3)_3\cdot 6H_2O$ was replaced by $Dy(NO_3)_3\cdot 6H_2O$. After about one week, colorless block crystals of **4** suitable for X-ray diffraction were obtained. Anal. Found for **4**: C, 4.16; H, 1.74; N, 2.20; Dy, 8.41; W, 55.92 (%); $C_{14}H_{64}N_6O_{68}Dy_2W_{12}$ (Mr=3935.46, 43.6% based on Dy) requires C, 4.27; H, 1.62; N, 2.13; Dy, 8.26; W, 56.06 (%). ν_{max}(KBr pellet) cm^{-1}: 3424.34(m), 1646.05(m), 1578.84(m), 1441.91(m), 1397.88(s), 1286.50(w), 1108.63(w), 937.77(s), 877.36(s), 782.69(s), 753.55(s), 422.47(w).

2.3. X-ray crystallographic study

The diffraction data of **1–4** were collected on a Bruker Smart CCD diffractometer with graphite-monochromated Mo*Kα* radiation (λ=0.71073 Å) at 293 K. Empirical absorption correction was

Table 1
Crystal data and structure refinements for compounds **1–4**.

Complex	1	2	3	4
Formula	$C_{14}H_{64}N_6O_{68}Eu_2W_{12}$	$C_{14}H_{64}N_6O_{68}Gd_2W_{12}$	$C_{14}H_{66}N_6O_{69}Tb_2W_{12}$	$C_{14}H_{64}N_6O_{68}Dy_2W_{12}$
Mr	3914.40	3924.96	3946.32	3935.46
Crystal system	Monoclinic	Monoclinic	Monoclinic	Monoclinic
Space group	*P*2(1)/*n*	*P*2(1)/*n*	*P*2(1)/*n*	*P*2(1)/*n*
a (Å)	12.9400(9)	12.9364(2)	12.9244(2)	12.9235(10)
b (Å)	25.0820(18)	25.0601(4)	25.0735(4)	25.122(2)
c (Å)	21.3411(15)	21.4429(5)	21.4621(4)	21.5695(17)
β (deg)	97.093(1)	97.401(2)	97.532(2)	98.149(1)
V ($Å^3$)	6873.5(8)	6893.6(2)	6895.0(2)	6932.1(9)
Z	4	4	4	4
D_c (g cm^{-3})	3.742	3.741	3.759	3.731
T (K)	296	293(2)	293	296
μ (mm^{-1})	21.910	21.951	22.076	22.071
F(000)	6824.0	6832	6872.0	6848.0
Measured refls	17331	18780	18929	17353
Obs reflns	10781	8015	9952	10844
R(int)	0.0763	0.0559	0.0570	0.0804
GOF on F^2	1.000	0.745	1.003	1.010
Final R_1[a], wR_2[b] [$I \geq 2\sigma(I)$]	0.0474, 0.0977	0.0350, 0.0490	0.0454, 0.0809	0.0514, 0.1147
Final R_1[a], wR_2[b] (all data)	0.0848, 0.1090	0.0858, 0.0516	0.0741, 0.0831	0.0877, 0.1330

[a] $R_1 = \Sigma\|F_o| - |F_c\|/\Sigma|F_o|$.
[b] $wR_2 = \{\Sigma[w(F_o^2 - F_c^2)^2]/\Sigma[w(F_o^2)^2]\}^{1/2}$.

applied. The structures were solved with the direct methods and refined with the full-matrix least-squares methods on F^2 using the *SHELXTL*-97 crystallographic software package [23,24]. The positions of hydrogen atoms on carbon atoms were calculated theoretically. A summary of the crystallographic data and structural determination for **1–4** is shown in Table 1.

3. Results and discussion

Single-crystal structural analyses reveal that compounds **1–4** are isomorphic with a polar space group $P2(1)/n$. Their unit cell dimensions, volumes, related bond distances and angles are changed (Table 1 and Table S1) according to the changing sequence of Ln^{3+} radii. The W_{12} cluster has α-Keggin type structure with a cuboctahedral shape (Oh symmetry), and has six square-shaped faces and eight triangle-shaped faces in which oxygen ligands link tungsten atoms by edge- or corner-sharing. The two hydrogen atoms of W_{12} occupy the center of the cluster.

3.1. Description of crystal structures

Compound **1** is taken as an example to depict their structures in detail. Every asymmetrical unit of **1** consists of one W_{12} cluster, two Eu^{3+} ions, two L^{2-} ligands and eleven water molecules. Two crystallographically independent Eu^{3+} ions (Eu1 and Eu2) locate in different coordination environments in **1** (Fig. 1). Eu1 ion is coordinated by nine oxygen atoms finishing its tricapped triprismatic coordination geometry (Fig. 2a), namely, three carboxyl oxygen atoms from two L ligands, five oxygen atoms from water molecules, and one terminal oxygen atom from the W_{12} subunit. Eight-coordinated Eu2 ion is surrounded by two carboxyl oxygen atoms from two different L ligands and two terminal oxygen atoms from two W_{12} clusters and four water molecules, showing a distorted bicapped triangular prism coordination geometry (Fig. 2b). Furthermore, two crystallographically independent pyridine-3,5-dicarboxylate ligands adopt two different coordination modes (μ_2, η^2, η^1) and (μ_2, η^1, η^1). L1 ligand coordinates to Eu1 and Eu2’ atoms in (μ_2, η^2, η^1) coordination mode (Scheme 1a) with a long Eu–O bond of 2.566(11) Å, that forming one chelate ring with Eu1 atom and bridging Eu2 atom in monodentate way. L2 ligand provides two oxygen atoms of two carboxyl groups to coordinate to Eu1′ and Eu2 atoms in (μ_2, η^1, η^1) coordination mode (Scheme 1b). Such connection creates a Eu–L polymeric chain (Fig. 3). The W_{12} cluster acts as a tridentate ligand which connects three Eu^{3+} ions (Eu1, Eu2 and Eu2′) with its three terminal oxygen atoms (Fig. 4a), resulting in a 14-numbered ring $W_2O_3Eu_2O_2C_5$ together with L1 ligand (Fig. 4b). Eu2 atom is coordinated by two W_{12} clusters as mentioned above so that a Eu–W_{12} polymeric chain is formed (Fig. 5). Eu–W_{12} chains and L–Eu chains form a two-dimensional (2-D) structure parallel to *ac* plane which exhibits a (7^2.3) (7^2.3)

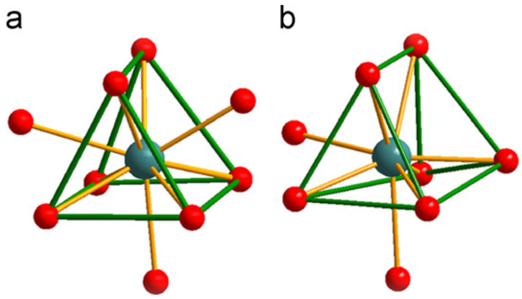

Fig. 2. The coordination geometries of *Ln* ions in **1**–**4**. The color codes are as follows: Ln^{3+} teal, O red (for interpretation of the references to color in this figure legend, the reader is referred to the web version of this article).

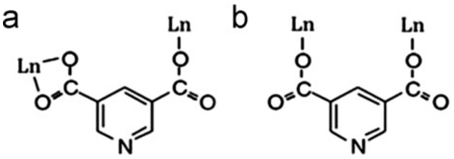

Scheme 1. Coordination models of the pyridine-3,5-dicarboxylic acid ligands.

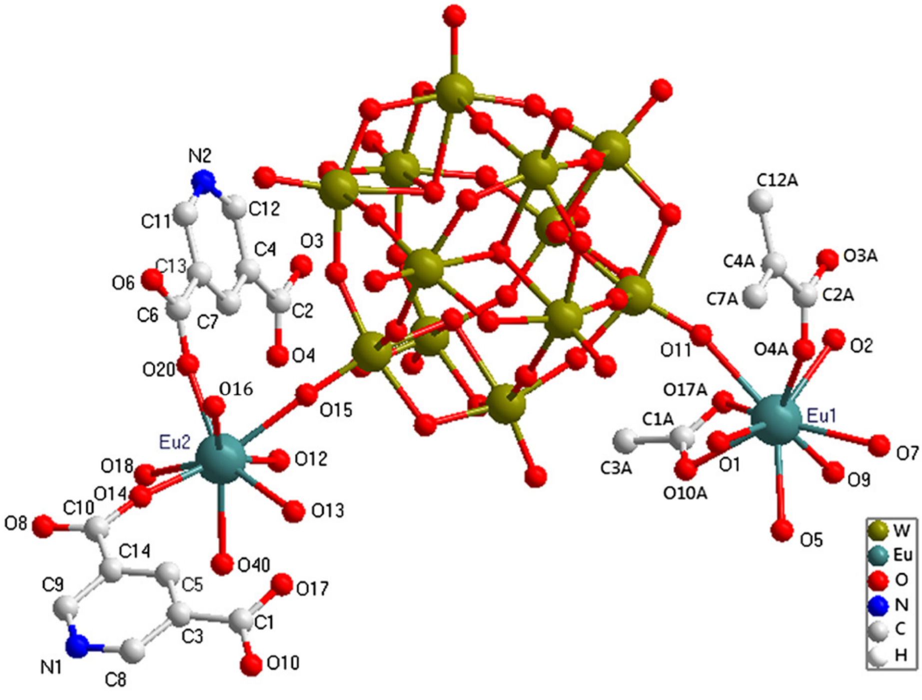

Fig. 1. ORTEP drawing of **1**. Lattice water molecules and hydrogen atoms have been omitted for clarity.

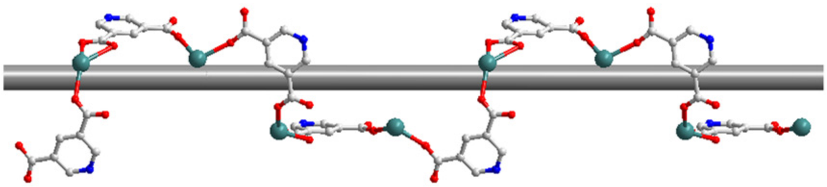

Fig. 3. Eu–L polymeric chain. The color codes are as follows: Ln^{3+} teal, O red, C gray, N blue, all hydrogen atoms and water molecules are omitted for clarity (for interpretation of the references to color in this figure legend, the reader is referred to the web version of this article).

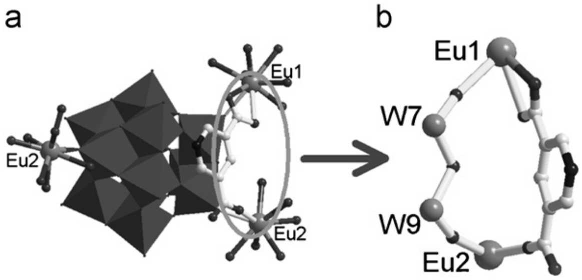

Fig. 4. (a) Polyhedral/ball/stick representation of three supporting subunit of W_{12} cluster. (b) 14-numbered ring $W_2O_3Eu_2O_2C_5$.

($7^5.11^2.3$) topology (Fig. 6) via sharing Eu2 atoms. Because of the existence of a lot of coordinated and lattice water molecules, there are multifold hydrogen bonds between the 2-D layers which leads to a three-dimensional architecture.

Comparing to pyridine-2,6-dicarboxylate, pyridine-3,5-dicarboxylate is lack of chelating ability so that it acts only as bridging ligand and the nitrogen atom does not take part in coordination in these compounds. That is, the coordination ability of pyridine-3,5-dicarboxylate is restrained by the big volume of the W_{12} cluster, the carboxyl group mainly acts as monodentate coordination unit. Compounds **2–4** have the similar structural features to **1**.

Based on bond valence sum calculations and charge balance consideration, all W and *Ln* centers exhibit the +6 and +3 oxidation states, respectively [25].

3.2. IR spectra

The IR spectra of compounds **1–4** are presented in Fig. S1. In compound **1,** the features at 936, 877, 781, 753 cm^{-1} are very typical for Keggin anions and should be attributed to ν(W–Ot), ν(W–Ob–W) and ν(W–Oc–W), respectively. Upon comparison of the IR spectrum of **1** with those of reference [26], it can be seen that the W–Oc–W vibration absorption band split into two bands (781 and 753 cm^{-1}). To explain this change we examined the anionic structure and found an obvious change in W–Oc–W angles. In general, the angle of W–Oc–W bond is about 120° and that of W–Ob–W bond is about 150° [26]. In **1**, the angles of W–Oc–W bonds are divided into two groups: 117–120° and 109–114° (Table S1). The latter group of angles is related to the tri-metal groups W_3O_{13} in which two terminal oxygen atoms coordinate to Eu1 and Eu2 ions. The Eu1 and Eu2 ions are bridged by a L ligand. It is the geometric limit of this bridging ligand L that makes angles of W–Oc–W bonds decrease and therefore the W–Oc–W vibration absorption band is split. That is, polyanions in **1** still retain the basic Keggin structure, but are distorted due to the effect of coordination.

The sharp band at 421.79 cm^{-1} should be attributed to Eu–O stretching vibration. The vibration absorption bands of L ligand appear in the region of 1100–1650 cm^{-1}, it is well known that the difference $\Delta\nu$ ($\Delta\nu = \nu_{as} - \nu_{sym}$), between the asymmetric stretching vibration and the symmetric one of the carboxyl group, depends on its coordination mode [27]. The ν_{as}(OCO) and ν_s(OCO) vibrations of the carboxyl groups of **1** are around 1575 and 1397 cm^{-1}, respectively. The $\Delta\nu$ value ($\sim$178 cm^{-1}) is close to the value expected for a di-monodentate-bridging coordination mode [28], which is consistent with the crystal structure of **1**. And the weak peaks at 1108–1286 cm^{-1} can be regarded as C–N, C–C stretching vibrations. The similar frequencies of the asymmetric and symmetric stretching vibrations of COO groups in different compounds point to the same coordination mode of carboxyl groups in these compounds. The peak at 1439 cm^{-1} can be regarded as being characteristic of the $n(NH_4^+)$ modes. The presence of water molecules in the structures of the compounds is confirmed by the bands centered at about 3424 and 1641(s) cm^{-1} arising from the stretching vibrations of OH groups engaged in hydrogen bonds. The IR spectra of compounds **2–4** are similar to that of **1**.

3.3. Thermogravimetric analyses

The TG analyses for compounds were carried out in the interest of studying the thermal behavior of polycrystalline samples in N_2. The TG curve of **1** (Fig. S2a) displays a four-step weight loss in the temperature range 40–900 °C. The weight loss of 10.71% from 40 to 305 °C is attributed to the loss of absorption, lattice and partial coordination water and NH_3 molecules. The weight loss of 5.84% corresponds to the loss of all coordinated water and decomposition of the ligands between 305 and 540 °C. At this period *Ln*–L–W_{12} compound had transferred to $Ln_2(CO_3)_3$ and WO_3. The IR data indicate that rare earth carbonate and tungsten trioxide as decomposing products with the absorption bands at 1579, 1385 cm^{-1} of CO_3^{2-} and 860 cm^{-1} of WO_3. At the temperature above 600 °C, $Ln_2(CO_3)_3$ decomposed and up to 800 °C the decomposition was completed. The fact that the total weight loss of 22.15% is larger than that calculated for $C_{14}H_{64}N_6O_{68}Eu_2W_{12}$ (20.0%) is due to the presence of absorption water molecules. Compounds **2** and **3** exhibit the similar thermal decomposition behaviors to that of **1**, the total weight loss of 20.02% and 21.29% (calculated values are 19.31% and 19.66%), respectively (Fig. S2b, c). The first two steps of **4** become a slow continuous weight loss process corresponding to the loss of absorption, lattice and coordination water and NH_3 molecules with the weight loss of 11.79% (calculation value is 10.88%) (Fig. S2d). At the temperature above 588 °C, it is the decomposition of ligands and transformation of oxalate to oxide with the weight loss of 8.48% (calculation value is 8.49%).

3.4. Photoluminescence

The luminescent properties of **1**–**4** were investigated in the solid state (Fig. 7). The emission spectra of **1**, **3**, **4** exhibit the characteristic emission of Eu(III), Tb(III) and Dy(III), respectively. Eu-**1** gives five characteristic peaks by exciting the crystal samples at 396.0 nm (Fig. 7a). The two stronger peaks are attributed to $^5D_0 \rightarrow {}^7F_1$ (593 nm), $^5D_0 \rightarrow {}^7F_2$ (618 nm) transitions

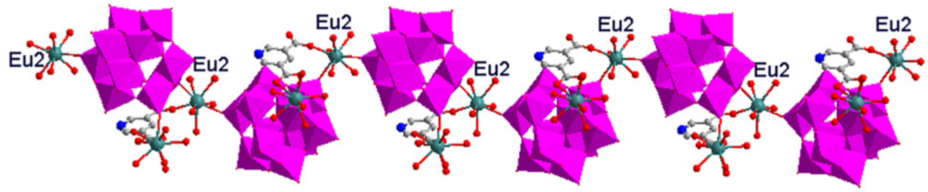

Fig. 5. Polyhedral/ball-and-stick representation of Eu–W_{12} polymeric chain. The color codes are as follows: Eu^{3+} teal, O red, C gray, N blue, all hydrogen atoms are omitted for clarity (for interpretation of the references to color in this figure legend, the reader is referred to the web version of this article).

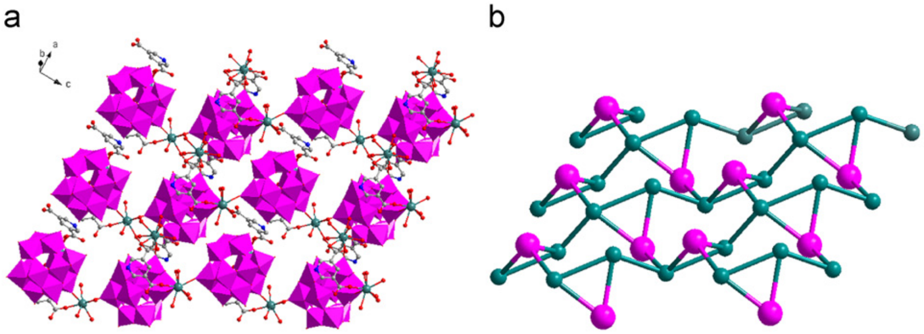

Fig. 6. (a) Polyhedral and ball-and-stick representation of 2-D layer framework of **1**. All hydrogen atoms and free water molecules are omitted for clarity. (b) Schematic view of (7^2.3) (7^2.3) (7^5.11^2.3) topology of **1**.

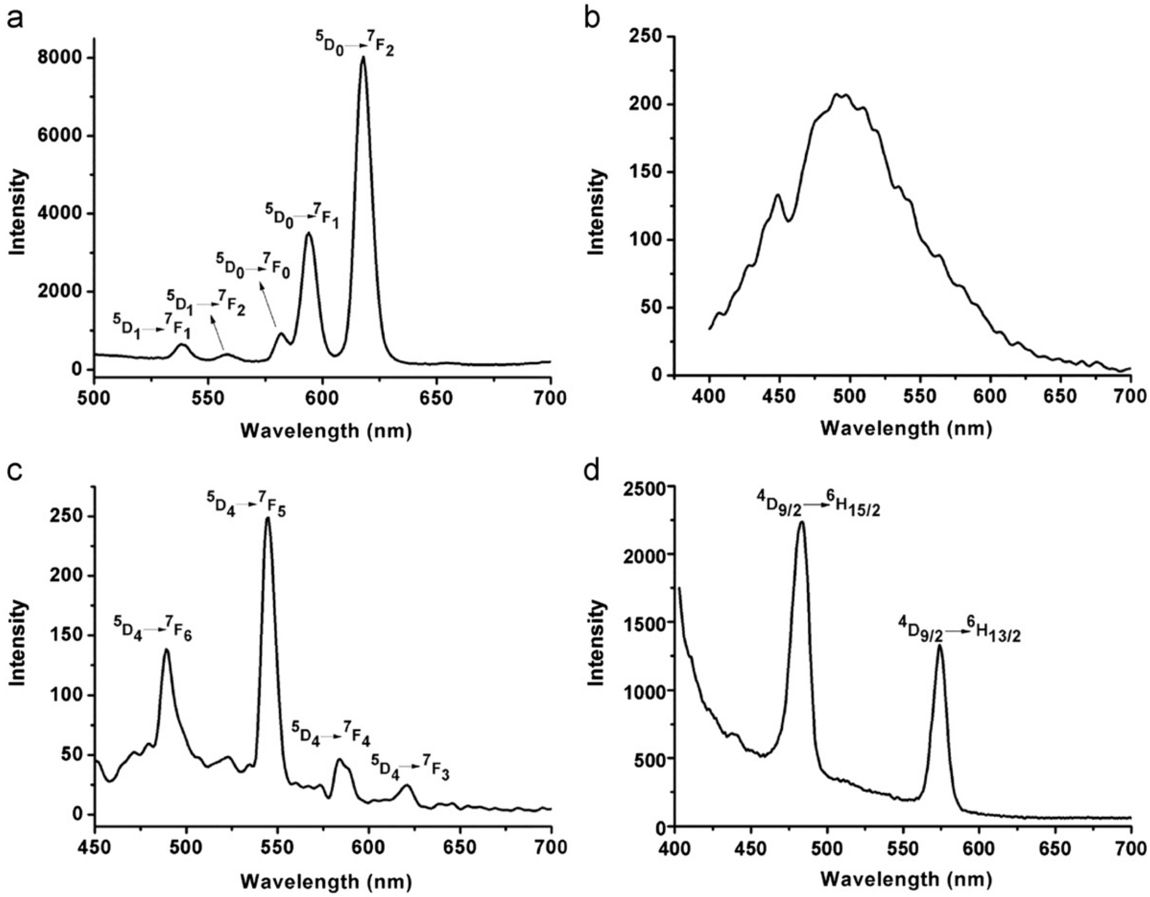

Fig. 7. Emission spectra of compounds **1–4**.

and the three weaker peaks belong to the transitions of $^5D_1 \rightarrow {}^7F_1$ (538 nm), $^5D_1 \rightarrow {}^7F_2$ (557 nm) and $^5D_0 \rightarrow {}^7F_0$ (581 nm) [29–31]. The intensity of the $^5D_0 \rightarrow {}^7F_2$ transition (electric dipole) of Eu(III) at 618 nm is stronger than that of the $^5D_0 \rightarrow {}^7F_1$ transition (magnetic dipole) at 593 nm, indicating that the coordination environment of the Eu(III) ion is asymmetric [32], which is confirmed by crystallographic analyses. The highest intensity of $^5D_0 \rightarrow {}^7F_2$ transition implies intense red luminescence of **1**. The appearance of the symmetry-forbidden emission $^5D_0 \rightarrow {}^7F_0$ (581 nm) indicates that Eu(III) ions in **1** occupy low symmetric sites and without an inversion center. This is in agreement with our single-crystal X-ray analysis. The emission spectrum of Tb-**3** is shown in Fig. 7c. Under the excitation at 291 nm, it produces four emission peaks at 489, 543, 583 and 620 nm, respectively, assigned to be the transition of Tb(III) ions from $^5D_4 \rightarrow {}^7F_J$ (J=6, 5, 4, 3) [33–36]. Compound **3** has intense and pure green luminescence and can be a good candidate for green-light emitting diode devices [37–38]. Dy-**4** shows two characteristic peaks in its emission spectrum under the excitation at 388.0 nm, which are attributed to transitions of $^4D_{9/2} \rightarrow {}^6H_{15/2}$ (482 nm) and $^4D_{9/2} \rightarrow {}^6H_{13/2}$ (574 nm) (Fig. 7d) of Dy atom. The fact that emission bands of the ligand molecules do not appear in the emission spectra of Eu, Tb and Dy compounds points to efficient transfer of the excitation energy from ligand to metal. Compound 2 displays pale fluorescence with a broad emission band at 450–550 nm (λ_{max}=479 nm) by exciting the crystal samples at 291 nm (Fig. 7b). The emission peaks exhibit obviously red-shift in contrast to the free ligand (H_2L) with a broad emission peak, which might be attributed to π–π* transition of ligand [39]. Therefore, we have the reason to believe that the coordination of the ligand to the metal centers in **2** should have no evident effect on the luminescence of the ligand.

4. Conclusions

In conclusion, the lanthanide compounds based on pyridine-3,5-dicarboxylate and W_{12} polyoxoanoins were successfully synthesized in aqueous solution and structurally characterized. Compounds **1–4** are isostructural with a 2-D grid. The carboxyl groups of pyridine-3,5-dicarboxylate provide two kinds of coordination ways, (μ_2, η^2, η^1) and (μ_2, η^1, η^1). Ring coordination of pyridine-3,5-dicarboxylate and W_{12} to *Ln* changes the bond angles of W_{12} that leads to splitting of vibration band of W–Oc–W. On the other hand, the compounds of Eu^{3+} (**1**), Tb^{3+} (**3**) and Dy^{3+} (**4**) exhibit characteristic lanthanide-centered luminescence. Furthermore, compound **2** exhibits a weak ligand-centered luminescence. Our research results indicate that W_{12} polyoxoanoins and *Ln* ions are good candidates for designing novel high-dimensional compounds with varying architectures and desired properties, and pyridine-3,5-dicarboxylate as a promising multifunctional ligand has a great potential in the field of coordination polymers.

Appendix A. Supporting information

Crystallographic information files (CIF) and IR, TG data. CCDC 800868, 803712, 800870, 800869 contain the supplementary crystallographic data for compounds **1–4**. These data can be obtained free of charge via http://www.ccdc.cam.ac.uk/deposit, or from the Cambridge Crystallographic Data Centre, 12 Union Road, Cambridge CB2 1EZ, UK; fax: +(44) 01223 336 033; or e-mail to deposit@ccdc.cam.ac.uk.

References

[1] J. Kido, Y. Okamoto, Chem. Rev. 102 (2002) 2357.
[2] N. Marques, A. Sella, J. Takats, Chem. Rev. 102 (2002) 2137.
[3] M.N. Bochkarev, Chem. Rev. 102 (2002) 2089.
[4] (a) S. Petoud, S.M. Cohen, J.-C.G. Bunzli, K.N. Raymond, J. Am. Chem. Soc. 125 (2003) 13324;
  (b) N. Ishikawa, M. Sugita, T. Ishikawa, S.Y. Koshihara, Y. Kaizu, J. Am. Chem. Soc. 125 (2003) 8694.
[5] C.M. Zaleski, E.C. Depperman, J.W. Kampf, M.L. Kirk, V.L. Pecoraro, Angew. Chem. Int. Ed. 43 (2004) 3912.
[6] T. Hamada, K. Manabe, S. Ishikawa, S. Nagayama, M. Shiro, S. Kobayashi, J. Am. Chem. Soc. 125 (2003) 2989.
[7] T. Devic, C. Serre, N. Audebrand, J. Marrot, G. Ferey, J. Am. Chem. Soc. 127 (2005) 12788.
[8] S.K. Ghosh, P.K. Bharadwaj, Inorg. Chem. 43 (2004) 2293.
[9] D.T. Lill, N.S. Gunning, C.L. Cahill, Inorg. Chem. 44 (2005) 258.
[10] (a) N. Sabbatini, M. Guardigi, F. Bolletta, I. Manet, R. Ziessel, Angew. Chem. Int. Ed. Engl. 33 (1994) 1501;
  (b) X.-P. Yang, R.A. Jones, J. Am. Chem. Soc. 127 (2005) 7686.
[11] (a) B.S. Harrison, T.J. Foley, A.S. Knefely, J.K. Mwaura, G.B. Cunningham, T.S. Kang, M. Bouguettaya, J.M. Boncella, J.R. Reynolds, K.S. Schanze, Chem. Mater. 16 (2004) 2938;
  (b) H.S. He, J.P. Guo, Z.X. Zhao, W.K. Wong, W.Y. Wong, W.K. Lo, K.F. Li, L. Luo, K.W. Cheah, Eur. J. Inorg. Chem. 4 (2004) 837;
  (c) D. Parkar, Coord. Chem. Rev. 205 (2000) 109;
  (d) A.H. Morrish, The Physical Principles of Magnetism, Wiley, New York, 1965.
[12] (a) R.S. Dickins, S. Gaillard, S.P. Hughes, A. Badari, Chirality 17 (2005) 357;
  (b) Y.M. Yao, Z.Q. Zhang, H.M. Peng, Y. Zhang, Q. Shen, J. Lin, Inorg. Chem. 45 (2006) 2175;
  (c) S.W. Wang, S.L. Zhou, E.H. Sheng, M.H. Xie, K.H. Zhang, L. Cheng, Y. Feng, L.L. Mao, Z.X. Huang, Organometallics 22 (2003) 3546;
  (d) S. Tobisch, J. Am. Chem. Soc. 127 (2005) 11979.
[13] (a) L. Pan, K.M. Adams, H.E. Hernandez, X. Wang, C. Zheng, Y. Hattori, K. Kaneko, J. Am. Chem. Soc. 125 (2003) 3062;
  (b) T. Gunnlaugsson, J.P. Leonard, K. Senechal, A.J. Harte, J. Am. Chem. Soc. 125 (2003) 12062.
[14] (a) K. Kuriki, Y. Koike, Y. Okamoto, Chem. Rev. 102 (2002) 2347;
  (b) H. Tsukube, S. Shinoda, Chem. Rev. 102 (2002) 2389.
[15] K. Fukaya, T. Yamase, Angew. Chem. Int. Ed. 42 (2003) 654.
[16] H.Y. An, D.R. Xiao, E.B. Wang, Y.G. Li, Z.M. Su, L. Xu, Angew. Chem. Int. Ed. 45 (2006) 904.
[17] X.L. Wang, C. Qin, E.B. Wang, Z.M. Su, Y.G. Li, L. Xu, Angew. Chem. Int. Ed. 45 (2006) 7411.
[18] A.X. Tian, J. Ying, J. Peng, J.Q. Sha, Z.G. Han, J.F. Ma, Z.M. Su, N.H. Hu, H.Q. Jia, Inorg. Chem. 47 (2008) 3274.
[19] (a) C.R. Sprangers, J.K. Marmon, D.C. Duncan, Inorg. Chem. 45 (2006) 9628;
  (b) D.L. Long, H. Abbas, P. Kogerler, L. Cronin, J. Am. Chem. Soc. 126 (2004) 13880;
  (c) R.N. Devi, E. Burkholder, J. Zubieta, Inorg. Chim. Acta 348 (2003) 150.
[20] M.X. Hu, Y.G. Chen, C.J. Zhang, Q.J. Kong, Cryst. Eng. Commun. 12 (2010) 1454.
[21] H.J. Pang, Y.G. Chen, F.X. Meng, et al., Inorg. Chim. Acta 361 (2008) 2508.
[22] J.H. Son, Y.U. Kwon, O.H. Han, Inorg. Chem. 42 (2003) 4153.
[23] G.M. Sheldrick, SHELX-97, Program for Crystal Structures Solution, University of Göttingen, 1997.
[24] G.M. Sheldrick, SHELX-97, Program for Crystal Structures Refinement, University of Göttingen, 1997.
[25] I.D. Brown, D. Altermatt, Acta Crystallogr. Sect. B Sci. 41 (1985) 244.
[26] J. Fuchs, E.P.Z. Flindt, Z. Naturforsch. B 348 (1979) 412.
[27] G.B. Deacon, R.J. Philips, Coord. Chem. Rev. 33 (1980) 227.
[28] K. Nakamoto, Infrared Spectra and Roman spectra of Inorganic and Coordination Compound, Wiley, New York, 1986.
[29] J. Xia, B. Zhao, H.S. Wang, W. Shi, Inorg. Chem. 46 (2007) 3450.
[30] Subha Viswanathan, Ana de Bettencourt-Dias, Inorg. Chem. 45 (2006) 10138.
[31] A.R. Ramya, M.L.P. Reddy, Alan H. Cowley, Kalyan V. Vasudevan, Inorg. Chem. 49 (2010) 2407.
[32] A.F. Kirby, D. Foster, F.S. Richardson, Chem. Phys. Lett. 95 (1983) 507.
[33] Z.Y. Li, G.S. Zhu, X.D. Guo, X.J. Zhao, Z. Jin, S.L. Qiu, Inorg. Chem. 46 (2007) 5174.
[34] X.P. Yang, R.A. Jones, J. Am. Chem. Soc. 127 (2005) 7686.
[35] D.A. Chengelis, A.M. Yingling, P.D. Badger, C.M. Shade, S. Petoud, J. Am. Chem. Soc. 127 (2005) 16752.
[36] H. Xin, Y. Ebina, R. Ma, K. Takada, T. Sasaki, J. Phys. Chem. B 110 (2006) 9863.
[37] P.L. Li, Z.P. Yang, L.B. Pang, J. Rare Earths 26 (2008) 44.
[38] Mihail Nazarov, Do Young Noh, Jongrak Sohn, J. Solid State Chem. 180 (2007) 2493.
[39] J. Zhang, Z.J. Li, Y. Kang, J.L. Cheng, Y.G. Yao, Inorg. Chem. 43 (2004) 8085.